Institute for Advanced Science,
Social and Sustainable Future

MORALITY BEFORE KNOWLEDGE

An acetylcholinesterase-based biosensor of carbofuran using carbon foam electrode modified by graphene and gold particles

Respati K. Pramadewandaru[1],*, Sulis Triani[2], Yudhistira Tesla[3], Afiten Rahmin Sanjaya[2]

[1] *Department of Materials and Metallurgical Engineering, Faculty of Industrial Technology and System Engineering, Sepuluh Nopember Institute of Technology, Surabaya, East Java 60111, Indonesia;*

[2] *Department of Chemistry, Faculty of Mathematics and Natural Sciences, Universitas Indonesia, Depok, West Java 16424, Indonesia;*

[3] *Singota Solutions, Bloomington, Indiana 47401, United States.*

*Correspondence: respatikevin@its.ac.id

ABSTRACT

Background: This study introduces a novel acetylcholinesterase (AChE)-based biosensor for the sensitive and selective detection of carbofuran, a widely used carbamate pesticide known for its neurotoxicity. **Methods:** The biosensor employs a carbon foam (CF) electrode modified with graphene oxide and gold nanoparticles (CF/Graphene/Au), leveraging the synergistic properties of these materials to enhance electrochemical performance. Carbofuran detection is achieved through its inhibitory effect on AChE activity, monitored via cyclic voltammetry of thiocholine oxidation. **Findings:** Under optimal conditions at pH 7.4, the biosensor demonstrated a linear detection range of 25–125 µM, a detection limit of 8.08 µM, and a sensitivity of 0.3874 mA µM^{-1} cm^{-2}. It also showed strong reproducibility with a relative standard deviation of 6.77%. When tested on real vegetable samples, the biosensor achieved recovery rates between 88.95% and 111.30%. **Conclusion:** Compared to existing biosensor technologies, the CF/Graphene/Au-based sensor offers a well-balanced performance in terms of sensitivity, detection range, and practical usability. It presents a viable and portable solution for monitoring pesticide residues in environmental samples. **Novelty/Originality of this article:** This work presents a promising, portable solution for environmental monitoring of pesticide residues, integrating advanced nanomaterials and computational validation to improve detection accuracy and reliability.

KEYWORDS: acetylcholinesterase; Au; carbofuran; carbon foam; graphene.

1. Introduction

Pesticides are chemical substances which applied for controlling, repelling and exterminating pests. Among different groups of pesticides, carbamate pesticides have been widely used in many sectors of agriculture due to its' outstanding insecticidal activity and relatively low environmental persistence (Cai & Du, 2008; Singh et al., 2020; Zhang et al., 2006). The insecticidal activity of carbamate pesticides is related to their ability to inhibit an enzyme that catalyzes the hydrolysis reaction of acetylcholine (Zhang et al., 2006; Wei et al., 2014; Dhull et al., 2013; Bhuvanagayathri et al., 2020; Nunes et al., 2022; Cui et al., 2018; Yao et al., 2019; Fukuto, 1990). Besides its benefit to protect plants from pests, carbamate pesticides can cause various health problems for humans since they could be absorbed into

the soil and contaminate the water, as well as fruits and vegetables. Therefore, the determination of pesticide content in the environment holds significant importance. Conventional methods such as High Performance Liquid Chromatography (HPLC) (Prasad et al., 2013) and Gas Chromatography-Mass Spectrometry (GCMS) (Zhang et al., 2006) are commonly used for the determination of carbamate pesticides. However, those methods require difficult sample preparation, expensive equipment, and a competent operator (Dhull et al., 2013). Consequently, studies on the development of simpler, portable, cheap, fast, and selective carbamate pesticide sensors are still intensively studied.

On the other hand, electrochemical sensors are highly used in environmental monitoring due to their advantageous characteristics, including fast response times, high sensitivity, and cost-effectiveness (Akyüz & Koca, 2019; Eprilia et al., 2024; Fatah et al., 2024). Molecular recognition elements, such as antibodies, peptides, and enzymes, are extensively utilized in the sensors for electrochemical approaches. Notably, enzyme-based electrochemical sensors, such as those relying on acetylcholinesterase (AChE), are commonly selected to enhance the detection sensitivity of pesticides (Rachmawati et al., 2023; Pino et al., 2015). However, challenges related to biocompatibility, stability, and constraints in signal transmission mechanisms limit their efficacy as sensing tools. As a result, there is a pronounced focus on intensively investigating the development of robust and responsive pesticide sensors using various functional materials that address those issues.

Carbon-based material such as graphene is a 2D material composed of single-layer sheets of sp^2-bonded carbon atoms, packed into a honeycomb lattice that has a large surface area, high ion mobility, good conductivity, and stability (Singh et al., 2020; Buglione et al., 2012; Sookhakian et al., 2021; Ma et al., 2014; Baek et al., 2020; Nahda et al., 2025). Composite materials based on graphene and metal nanoparticles are very promising for biosensors because of their biocompatibility and their ability to enhance the selectivity and sensitivity of biosensors (Dhull et al., 2013; Bhuvanagayathri et al., 2020; Nunes et al., 2022; Cui et al., 2018; Rahmawati et al., 2022; Pundir & Chauhan, 2012) due to their fast electron transfer and large surface area. Among various metal nanoparticles, gold particles show a good performance in electrochemical sensors because of their large surface area, good adsorption ability, high conductivity, and provide good binding sites to maintain the bioactivity of biomolecules (Zahirifar et al., 2019). The combination of graphene and gold nanoparticles provides a synergistic effect of each material, resulting in a sensitive and selective biosensor (Rahmawati et al., 2022; Khalil et al., 2016; Ostadakbari et al., 2021). On the other hand, carbon foam (CF), which is a porous carbon material with a 3D structure, has good chemical stability, large surface area, good mechanical strength, and good conductivity, which make it suitable to be a supporting electrode material in electrochemical sensor (Olkhov & Shaw, 2014; Sanjaya et al., 2023). The 3D structure of CF is very beneficial for electron transfer due to its large porosity. Therefore, modification with graphene and Au particles into the surface of CF could help the electrode to form a higher surface area, which could escalate its ability to detect or oxidize thiocholine (Yao et al., 2019; Ostadakbari et al., 2021; Olkhov & Shaw, 2014; Ivandini et al., 2012; Jirasirichote et al., 2017). In this study, an enzymatic biosensor using CF modified with graphene and gold particles as the electrode was prepared for carbofuran detection. The evaluation of the prepared biosensors by using the cyclic voltammetry technique satisfactorily demonstrated the stability and low limit detection (LOD) for the detection of carbofuran.

2. Methods

2.1 Materials and apparatus

Acetylcholinesterase (AChE), acetylthiocholine iodide (ACTI), carbon foam, graphite rod, $HAuCl_4$, $NaBH_4$, $Na_3C_6H_5O_7$, $(NH_4)_2SO_4$, $NH_3.H_2O$, carbofuran, as well as KH_2PO_4 and K_2HPO_4 were purchased from Merck Sigma Aldrich. The phosphate buffer saline (PBS) was prepared from KH_2PO_4 and K_2HPO_4. Milli-Q water (18.2 MΩ cm) was used to obtain all the

solutions in this study. The instruments used were scanning electron microscopy–energy dispersive X-Ray (SEM-EDX, Hitachi SU-3500) and Raman spectroscopy (HORIBA iHR320). The electrochemical measurements were performed using Dropsens (DRP-STAT400) with a three-electrode system where the prepared electrode, Ag/AgCl system, and platinum wire were used as working, reference, and counter electrodes, respectively.

2.2 Synthesis of graphene-gold modified carbon foam (GrOx-Au@CF)

Graphene-modified carbon foam GrOx@CF was synthesized using modified electrochemical exfoliation of graphite (Dong et al., 2019). A two-electrode system was used with a piece of carbon foam and a graphite rod employed as the cathode and the anode, respectively. A solution containing $(NH_4)_2SO_4$ 0.1 M and $NH_3.H_2O$ 0.1 M was used as the electrolyte. Then, a current voltage of 8.0 V was applied to this system for 1 h to form graphene-modified CF (GrOx@CF). Afterwards, the obtained GrOx@CF was dried at room temperature. To prepare the graphene-gold modified carbon foam (GrOx-Au@CF), the prepared GrOX@CF was immersed in gold nanoparticle solution for 20 min and then dried at 60°C (Yao et al., 2019).

2.3 Preliminary study of carbofuran interaction with AChE and ACTI using molecular docking simulation

Molecular docking was performed using the covalent docking method in Molecular Operating Environment 2015.10 (MOE 2015.10). All the compounds used in this study are available online from (https://pubchem.ncbi.nlm.nih.gov) and (https://www.rcsb.org/). The structure of the AChE enzyme was obtained by removing ligand and water molecules on the crystal structure of AChE from the Protein Data Bank (PDB Code: 1AMN), then the polar hydrogen atoms were added to the amino acid residues. AChE structure was prepared using AMBER 10:EHT force field, while the ligands were prepared using MMFF94x force field. For the molecular docking simulation, the amino acid residue Ser200 was selected as a binding site for the ligands. Ten poses obtained from this simulation with the most negative values of Gibbs energy were observed (Ribeiro et al., 2022; Khodadadi et al., 2019; Anggraini et al., 2023). Among these poses, the best pose was selected, which has an RMSD value of less than two.

2.4 Electrochemical study of carbofuran biosensor

The carbofuran concentration was determined by the inhibition of AChE activity to the ACTI. The carbofuran was added to the electrolyte containing 50 mU AChE at pH 7.4. After 15 min, the solution was added with 25 μL ACTI solution. Then, after 10 min waiting time, cyclic voltammetry was conducted by applying potential ranged from -0.5 V to +1.0 V at the scan rate of 50 mV/s. The inhibition of carbofuran was then determined using the formula in eq 1.

$$\text{Inhibition (\%)} = (Ip;control - Ip;exp)/Ip;control \qquad \text{(Eq.1)}$$

2.5 Detection of carbofuran pesticides on the real sample

An amount of 0.5 grams of Pak choy vegetable that has been cut into small pieces are dissolved in 10 mL of methanol. The mixture was ultrasonicated for 15 min, followed by centrifuged for 15 min at 3000 rpm before supernatant was collected (Dong et al., 2019). The analysis of carbofuran was carried out using this supernatant using standard addition method. The measurements of carbofuran pesticide were validated using HPLC.

3. Results and Discussion

3.1 Preparation of GrOX@CF

GrOX@CF was prepared using electrochemical exfoliation methods on the surface of carbon foam (1 cm²). A graphite rod was exfoliated into graphene sheets due to the presence of anions (OH^- and SO_4^-) and gases (SO_2, O_2, etc) to help the intercalation process of the graphite layers (Ma et al., 2016). The exfoliated graphene sheet adsorbs NH_4^+ to be electrically attracted and assembled on the surface of cathodic CF. The resulting graphene structure does not completely coat the carbon foam's surface, leading to the interaction of X-rays with the underlying nickel layer. Consequently, the XRD pattern of CF (Fig. 1.a) only shows peaks at 44.5°, 51.8°, and 76.3° which represented nickel (111), (200), and (222), respectively. Most recent reported works exposed specific peak at 10° on the graphene oxide materials with lattice crystal (001). Whereas the XRD pattern of CF/Graphene shows a broad peak at 14° which are caused by the thin layer formation of graphene oxide, this shifting peak also found at 38° which represented carbon (100) as the contribute of unfinished oxidation graphene materials and also the deflect structure of thin layer graphene caused by the addition Au particles on the graphene structure (Ma et al., 2017). This might be due to the carbon layer that forms on the surface of nickel foam becomes thicker after modification with graphene sheets.
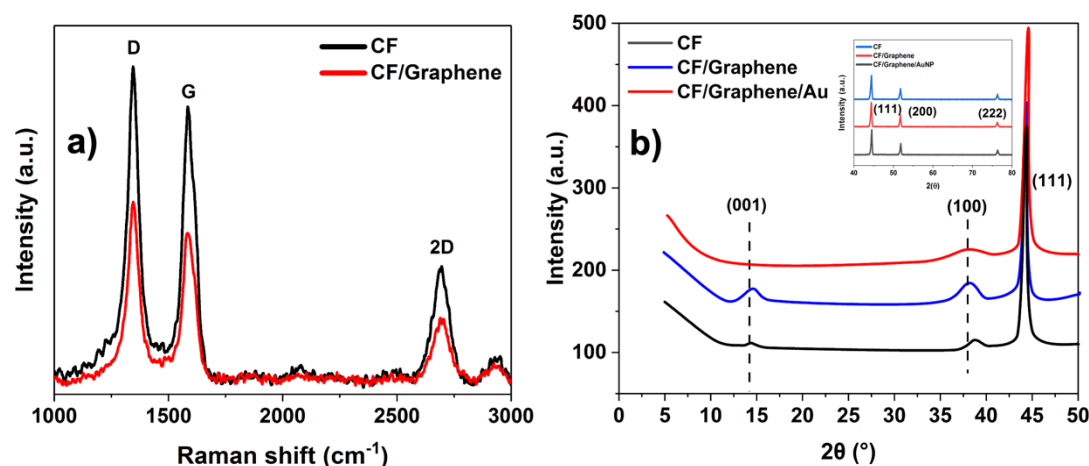

Fig. 1. Characterization of the modified electrode using (a) Raman spectroscopy; (b) XRD

Raman spectrum of CF and CF/Graphene presents 3 peaks; D, G and 2D band at 1348, 1590, and 2689 cm⁻¹, respectively (Fig. 1.b). The G peak appears due to the vibration of the carbon with sp^2 hybridization. The D peak indicates the defect in the sp^2 carbon structure, while the 2D peak represents the overtone of the D peak (Baek et al., 2020; Wang et al., 2014). The intensity ratio (ID/IG) was 1.16 and 1.19 for CF and CF/Graphene, which were similar to synthesized rGO by using chemical, electrochemical, and thermal methods (Baek et al., 2020; Wang et al., 2014). Insignificant changes in ID/IG might occur due to defects in the sp^2 structure of graphene sheets formed by oxidation during electrochemical exfoliation of the graphite rod. This is further confirmed by the EDX result (Table 1.) shows an increase of O atoms after modification with graphene sheets.

Table 1. EDX point characterization of the modified electrode

Material	Element (% Weight)			
	C	O	Ni	Au
CF	61.45	11.85	25.99	–
CF/Graphene	67.06	21.81	10.11	–
CF/Au	72.40	10.76	16.26	0.57
CF/Graphene/Au	69.64	8.59	19.70	2.06

SEM analysis was employed to examine the morphology of the prepared electrode. Fig. 2.a-b displays the SEM image of CF, revealing a smooth surface which covered by graphene sheets shaped like a ribbon attached onto the CF surface. The surface of the CF became rougher, and the graphene Fwrinkles were not formed, indicating that some of the graphene sheets were restacked on the surface of the carbon foam. The SEM images of CF/Graphene/Au (Fig. 2.c & d) show the presence of Au, indicating that Au particle have successfully deposited onto the CF/Graphene's surface. This observation was additionally supported by the EDX analysis (Table 1.), which revealed a weight percentage of 2.06% for Au.
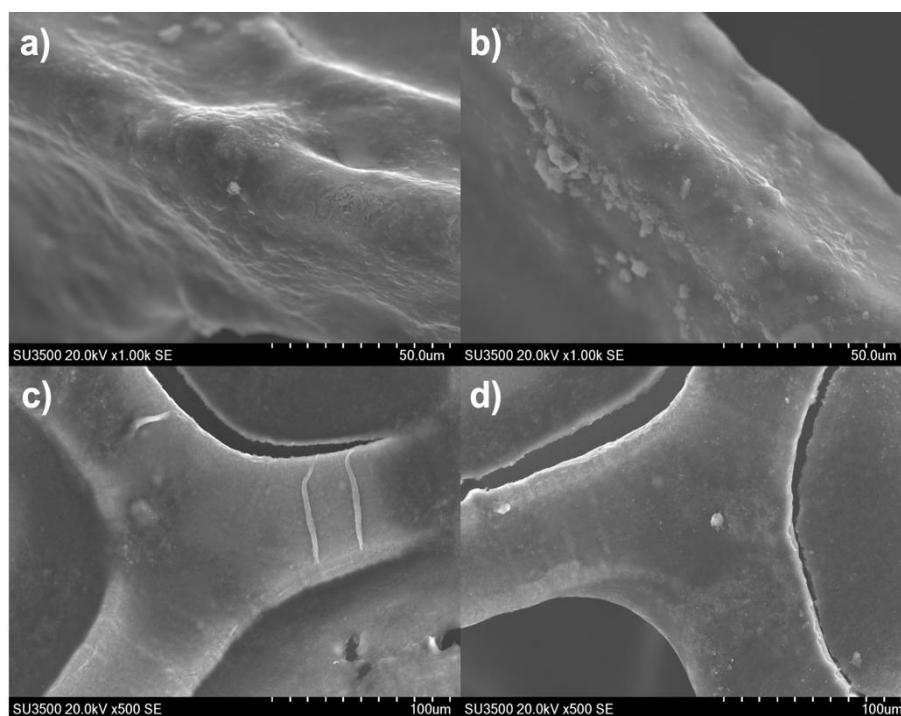

Fig. 2. SEM images of (a) CF; (b) CF/graphene; (c) CF/Au; (d) CF/graphene/Au

3.2 Molecular docking simulation of carbofuran interaction with AChE and ACTI

The binding modes of carbofuran and other evaluated compounds to AChE were studied using the covalent docking method (MOE 2015.10). Amino acid residue Ser200 was selected as the active site of AChE. Molecular docking simulations were performed by the induced-fit model, where the receptor could change its binding modes according to the shapes and binding modes of the ligands. As shown in Fig. 3., carbofuran forms a complex with AChE by covalent bonding of the carbamoyl moiety and amino acid residue Ser200. The AChE-Carbofuran complex is stabilized by hydrogen bonds between the carbonyl oxygen and amino acid residue in the oxyanion hole (Gly 118, Gly119, and Ala201). Inhibition of carbofuran to the AChE depends on the reaction conditions, such as pH. Hence, in this study, molecular docking simulations were performed at various pH conditions. As shown in Table 2., the lowest $\triangle$G binding value is obtained at the pH of 7.4, indicating that the most stable AChE-Carbofuran complex was formed at the pH of 7.4.

Table 2. Docking scores of AChE-Carbofuran with variation in pH

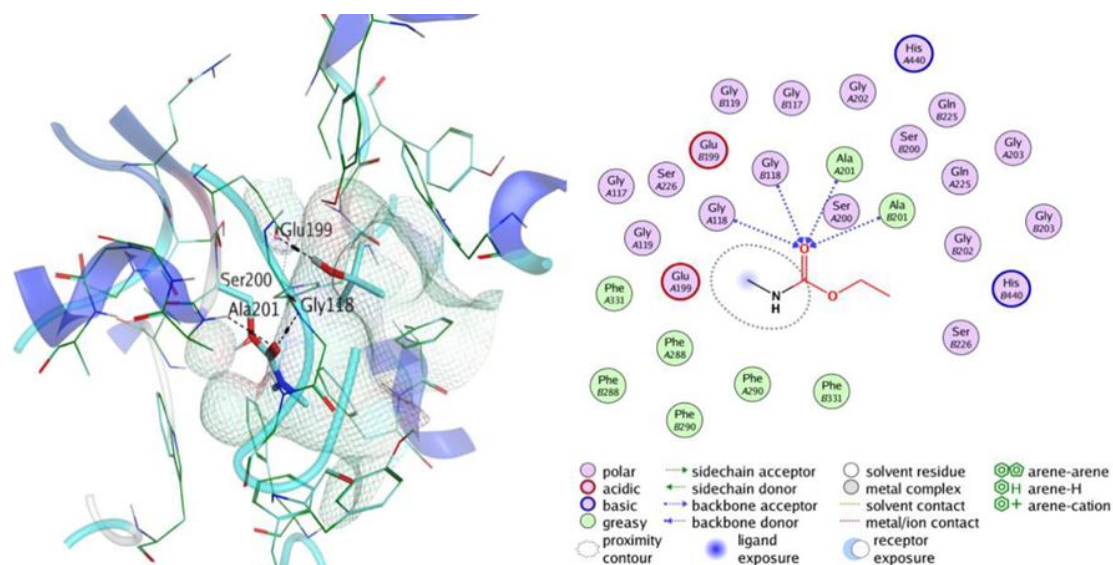| No	pH	ΔG binding (kcal/mol)	pKd
1	7.0	-3.9583	2.8835
2	7.2	-4.3332	3.1566
3	7.4	-4.6441	3.3831
4	7.6	-4.4029	3.2074
5	7.8	-4.4924	3.2726
6	8.0	-3.9733	2.8944

Fig. 3. Structure of AChE-Carbofuran complex and the molecular interaction as obtained from covalent docking into AChE (1AMN) at the pH of 7.4

In this study, molecular docking simulations were performed between AChE and other N-methyl carbamate compounds that are commonly used as active ingredients in pesticides (Table 3.). All of these compounds form a complex with AChE and the carbamoyl moiety is oriented toward the oxyanion hole (Gly118, Gly119, and Ala201). The stability of the AChE-Inhibitor complex can be observed by a dissociation constant (pKd). The dissociation constant can be determined as the tendency of a complex to dissociate into its constituent components. A higher pKd value indicates that the complex formation takes place spontaneously and the complex formed has good stability (Díaz & Peinado, 1997). AChE-Carbofuran complex has the greatest dissociation constant, hence, carbofuran forms the most stable complex with AChE. This indicates that the inhibition of carbofuran on the catalytic activity of AChE is greater than the other evaluated compounds.

Table 3. Docking scores of AChE-Inhibitors (N-methyl carbamate)

No	Carbamate compound	ΔG binding (kcal/mol)	pKd
1	Propoxur	-4.0676	2.9631
2	Carbaryl	-3.6352	2.6481
3	Fenobucarb	-4.3800	3.1907
4	Methiocarb	-4.3558	3.1731
5	Bendiocarb	-4.4683	3.2550
6	Terbam	-4.4822	3.2652
7	Carbofuran	-4.6441	3.3831

Based on the computational data, the inhibition mechanism of ACTI and AChE by carbofuran molecules was demonstrated in the Fig. 4., where the amino acid triads (serine, histidine, and glutamine) act as AChE active site (Ivandini et al., 2012). In a normal interaction between AChE and ACTI, the acetylation of the hydroxy site from the Ser200 proceeded by nucleophilic attack on the carbonyl site of ACTI. Another amino acid, such as Glu200 and His440 were playing an important role as a hydrogen donor or acceptor. The nucleophilic attack could generate the tetrahedral intermediate, which later will break C-O bonds to eliminate choline and generate acetylated AChE (Massoulie & Bon, 1982). In the presence of water, deacetylation of acetylated AChE produces acetic acid and free AChE. On the other hand, the presence of carbofuran molecules could inhibit the process by nucleophilic attack on the carbonyl group from the carbofuran molecules. By applying a similar mechanism, this inhibition process produces carbamylated AChE and carbofuran

phenol, thus decreasing the enzymatic reaction efficiency. As a result, the amount of thiocholine and acetic acid were also decreased.

a) Acetylcholine hydrolysis in the catalytic site of AChE
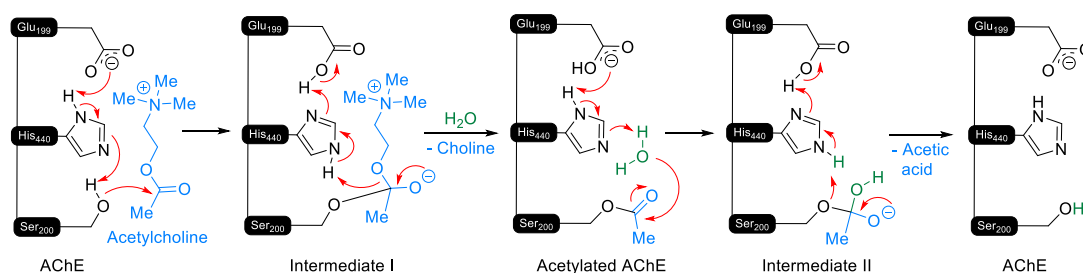
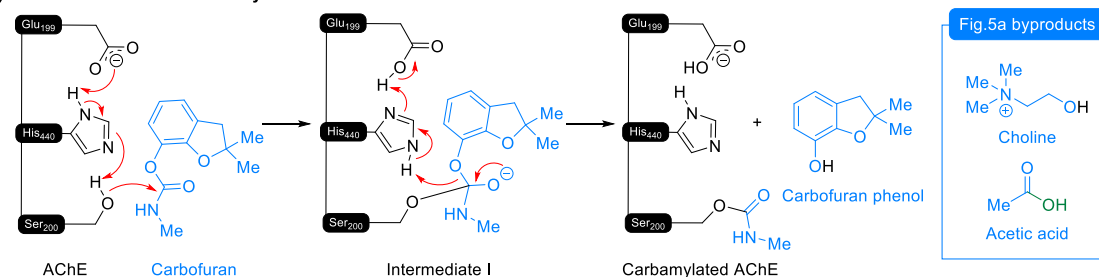**b) AChE inhibition mechanism by carbofuran**

Fig. 4. Proposed mechanism of (a) acetylcholine hydrolysis in the catalytic site of AChE; (b) AChE inhibition mechanism by carbofuran

3.3 Electrochemical behavior of the prepared electrode

The electrochemical behavior of the prepared electrode was studied compared with the unmodified CF in PBS pH 7.4 containing 1.0 mM ACTI and 50 mU AChE. The voltammograms at the potential range from -0.5 to +1.0 V in Fig. 5.a shows that the irreversible oxidation peak of thiocholine was observed at the potential of +0.55 V. The wrinkled structure of the graphene sheet at the surface of carbon foam could increase the active surface area of carbon foam. An oxidation peak of thiocholine shifted to the lower potential on the CF/Graphene/Au electrode and it produce the higher current response compared to another electrodes. This indicates that the presence of Au on the carbon layer could support to accelerate the electron transfer rate by stabilize the diffusion layer between the electrode surface and electrolyte system. These phenomena cannot be found on the CF/Au electrode, even though the Au particle is conductive materials the absence of graphene layer on the CF/Au makes the thickness of diffusion layer affected the charge transfer mechanism and interfere the stability of pesticides sensor measurement.

Furthermore, the behavior of CF/Graphene/Au was studied in the PBS solution in the presence and absence of ACTI, AChE, and carbofuran. Fig 5.b shown that the oxidation peak of thiocholine increased in the presence of AChE, this is because the enzyme was hydrolyzed the acethylthiocholine into thiocholine and acetic acid. Meanwhile, carbofuran in the systems decrease the oxidation peak of thiocholine, because the existence of carbonyl groups from the carbofuran residues interact with the Ser200 amino acid as active site of AChE, makes the ACTI oxidation to thiocholine and acetic acid was inactive.

The hydrolysis reaction of ACTI by AChE depends on the solution's pH. Regarding Fig 4.a the active site of AChE consists of serine, histidine, and glutamine (Ivandini et al., 2012). Histidine and glutamine could be ionized at the pKa 6 and 8, showing the best catalytic activity at the range of neutral pH. Therefore, study of the pH system was varied from 7.2 – 7.8. Fig. 6.a shows that the current density of thiocholine was increased from pH 7.2 to 7.4 and experience decline in oxidation peak current after that, this maybe the pH of enzyme to work in the high activity. The pH of system was main parameter that must be optimized to eliminate the enzyme deformation such a denaturated and dissociation molecules which

affected the enzyme performance. At physiological pH 7.4, the catalytic triad of acetylcholinesterase (AChE) consisting of Ser200, His440, and Glu199 exhibited optimal performance. This was confirmed by the highest observed pKd value using MD were listed on the Table 2, suggesting strong and stable enzyme–ligand interactions.
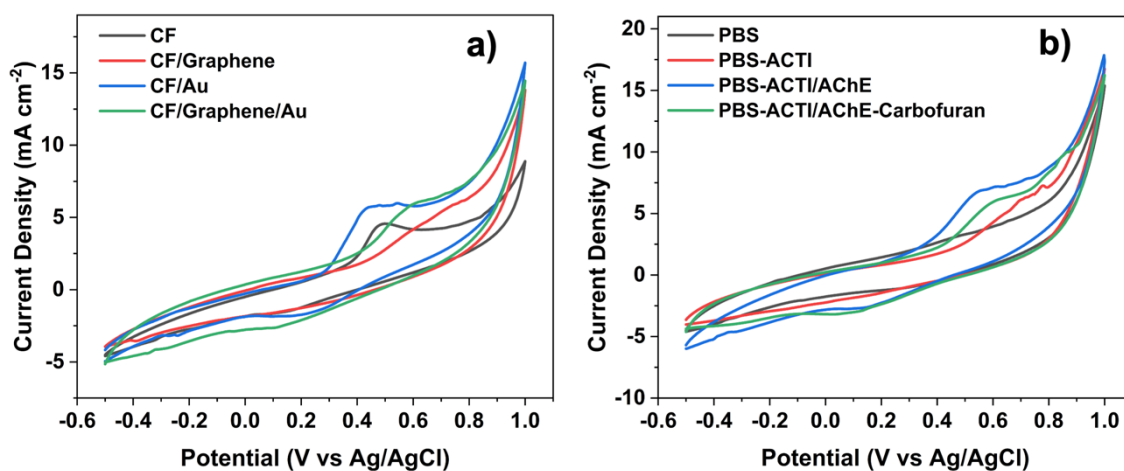

Fig. 5. Cyclic voltammogram of (a) PBS buffer pH 7.4 containing 1.0 mM ACTI and 50 mU AChE at CF, CF/Graphene, CF/Au and CF/Graphene/Au electrode; (b) in the PBS pH 7.4 solution in the presence and absence of ACTI, AChE, and carbofuran

The pH sensitivity of this triad, especially Ser200 and His440, plays a critical role in maintaining the nucleophilic and acid-base dynamics required for catalysis. However, as the pH increased beyond 7.6, the elevated concentration of OH^- ions began to interfere with the protonation balance of the active site residues. This disrupted the catalytic mechanism of the triad, resulting in a marked decrease in pKd values, which correlates with weakened binding and reduced enzymatic activity.

Interestingly, at pH 7.8, a subtle increase in pKd was observed, despite the general decline in triad activity. This anomaly is attributed to the activation of Ala201, a residue located near the catalytic triad but not directly involved in catalysis. Under specific structural and electrostatic conditions particularly involving interactions among acetylcholine ACTI, AChE, and carbamate inhibitors Ala201 appears to contribute to enhanced ligand binding, possibly by stabilizing the transition state or forming additional hydrogen bonds. Unlike the core catalytic residues, Ala201 is not pH-sensitive, but becomes functionally significant only in certain conformational states of the enzyme–ligand complex. This observation suggests a dual binding mechanism, where classical triad activity dominates under optimal pH conditions, while peripheral residues like Ala201 may assist under slightly alkaline conditions, possibly as a compensatory interaction site when the primary catalytic residues are less effective.

The variation concentration of molecular recognition AChE was studied in order to determine the concentration optimum of enzyme to produce sensor system with high effectivity and efficiency on the reagent used. Fig. 6.b shows that AChE concentration increases, higher production of thiocholine is obtained, and rise the peak to a certain concentration where the AChE converted all of the ACTI into thiocholine. After it reaches the maximum concentration, the peak current decreases or remains. Because, at a high concentration of enzyme, it will increase the diffusion layer that proportion to decrease the charge transfer performance. Fig. 6.b shows that the maximum peak current occurs when the concentration of AChE is 50 mU when the concentration was varied from 25 – 125 mU. Hence, 50 mU was chosen as the optimum concentration of AChE for the thiocholine measurement.

The contact time between AChE and ACTI was also observed in this study in the range of 5 – 25 minutes. The maximum peak current occurs when the contact time between AChE and ACTI is 10 minutes (Fig. 6.c). This might happen because all of the ACTI in the system

had converted into thiocholine. Inhibition time between AChE and carbofuran is also a key factor that could affect the performance of biosensors for pesticide detection. The presence of carbofuran help to reduce the thiocholine peak current (Jirasirichote et al., 2017). Therefore, the optimum inhibition time is determined by the largest decrease of the peak current.

Fig. 6.d shows that after 15 minutes of incubation, there is no significant decrease of the peak current. Thus, 15 minutes was chosen as the optimum inhibition time between AChE and carbofuran. Based on Fig. 4.b the carbofuran inhibits the hydrolysis reaction of ACTI into thiocholine by covalently binding to the serine residue in the catalytic triad of AChE (Wei et al., 2014; Pundir & Chauhan, 2012). Consequently, less thiocholine is produced, and its peak current decreases.
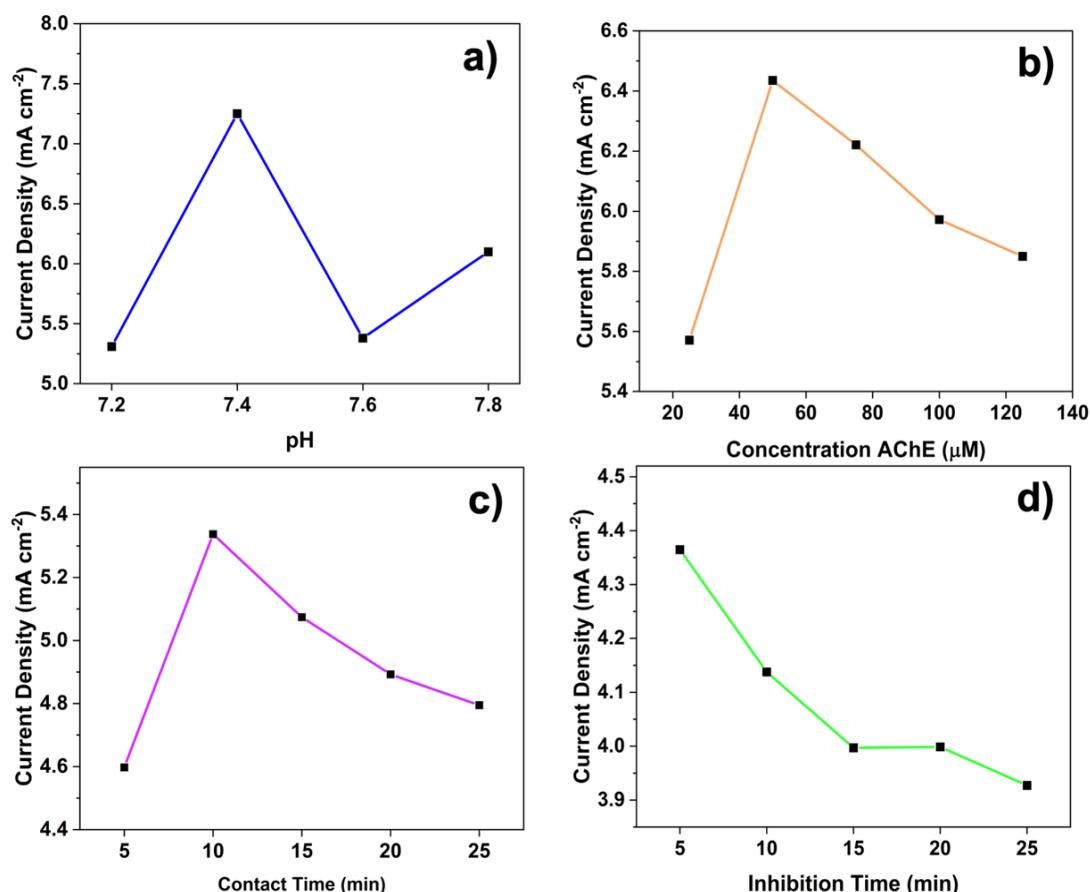

Fig. 6. The dependence of the current density on the CF/Graphene/AuNPs surface of PBS buffer pH 7.4 containing 1.0 mM ACTI and 50 mU AChE at the potential range of -0.5 – (+1 V)at various (a) pH; (b) AChE concentration; (c) contact time; (d) inhibition time

Fig. 7 a. and b show that the peak current decreases as the concentration of carbofuran increases under the optimum condition, with a good linearity between the concentration of carbofuran and the inhibition (Δ current response) in the range of 25 – 125 μM. The linear regression equation was $y = 0.3982x – 1.0733$. The limit of detection (LOD) was found 8.08 μM with a sensitivity of around 0.39 mA μM^{-1} cm^{-2}. Table 4 presents a comparison of the CF/Graphene/AuNPs sensor developed in this work with other reported biosensor electrodes. The proposed sensor demonstrates a limit of detection (LOD) of 8.08 μM and a linear detection range of 25–125 μM, which places it in the mid-performance tier among the compared systems. While it does not reach the ultra-high sensitivity of MWCNTs/AuNPs–CHIT/GCE (LOD: 0.01 μM) or CdS-decorated graphene (LOD: 0.34 μM), it significantly outperforms traditional materials such as Sol-gel/TMOS (LOD: 71.59 μM) and Au–PtNPs/GCE (LOD: 40 μM). Importantly, the CF/Graphene/AuNPs sensor offers a wider linear range than most high-sensitivity systems, making it more suitable for detecting

moderate-to-high analyte concentrations, such as typical pesticide residues in real samples. This makes it a highly applicable and efficient sensor design, especially for field-deployable or routine environmental analysis.
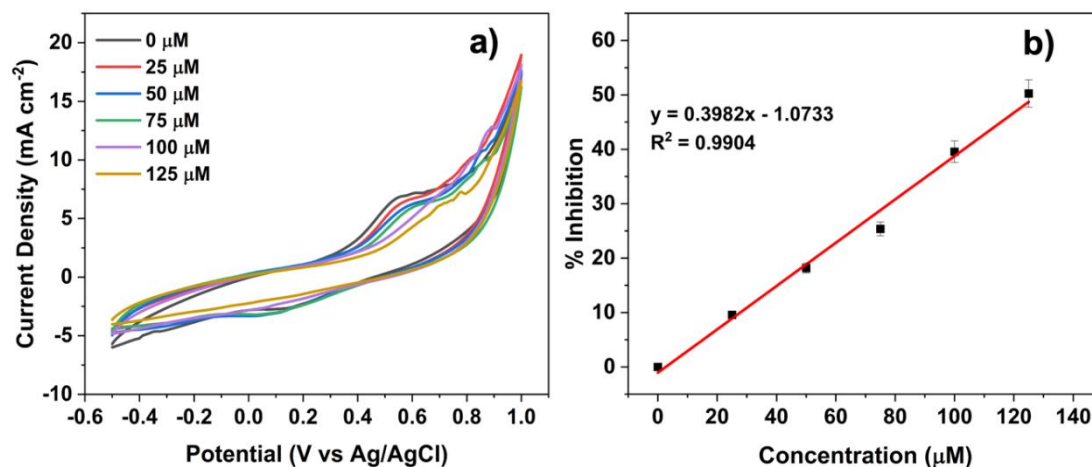

Fig. 7 (a) various concentration; (b) linearity

Table 4. Comparison develops biosensors with others substrate electrodes

Electrodes	Linear range (µM)	LOD (µM)	Ref
Sol-gel/TMOS	25.2 – 1690	71.59	(Díaz & Peinado, 1997)
Au-PtNPs/GCE	40 – 60	40	(Upadhyay et al., 2009)
CdS-decorated graphene nanocomposite	0.001 – 9.90	0.34	(Wang et al., 2011)
MWCNTs/AuNPs- CHIT/GCE	0.1 – 10	0.01	(Chui et al, 2018)
CF/Graphene/AuNPs	25 – 125	8.08	This work

3.4 Stability performance of carbofuran detection using CF/Graphene/Au electrode

The repeatability test was carried out to study the stability of the CF/Graphene/Au electrode by measuring the same CV experiment 10 times. The precision of the biosensor can be observed by conducting repeated tests, where smaller RSD and deviation values obtained were indicating a better performance of the biosensor. The biosensor using CF/Graphene/AuNPs electrode showed a fairly good level of precision for carbofuran detection Fig. 8a and b, with %RSD 6.77%.
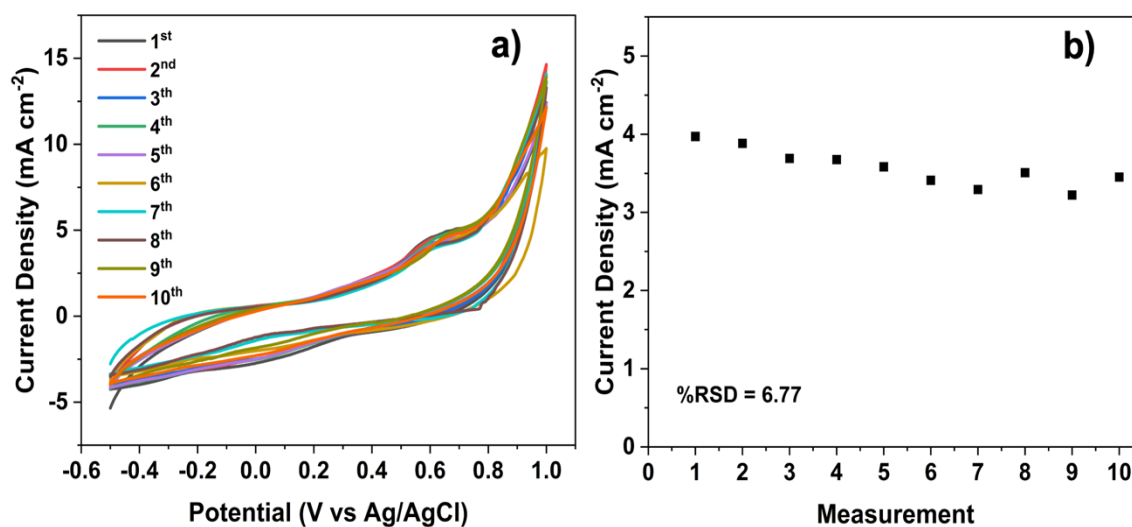

Fig. 8. Repeatability of developed biosensors

3.5 Application of modified electrode for detection of carbofuran pesticides in real samples

The potential practical application of enzymatic biosensors using CF/Graphene/Au electrodes for pesticide detection was studied by a recovery test. A recovery test was performed using the standard addition method by adding carbofuran standard into the *bhok coy* sample. The results in Table 4. show that the percentage of recovery is in the range of 88.95 – 111.3 %. This result indicates that the measurement of carbofuran in *bhok coy* could have interfered with other compounds or metabolites in the sample.

Table 5. Detection of carbofuran pesticides in the Bhok Coy real sample

Added (μM)	Detected		% Recovery	
	HPLC	Biosensor	HPLC	Biosensor
25	52.90	55.65	105.80	111.30
125	131.64	111.19	105.31	88.95

4. Conclusions

AChE biosensor has been successfully fabricated based on CF/Graphene/Au electrode for carbofuran detection. Detection of carbofuran was conducted by determining its inhibition toward the activity of AChE. Greater inhibition produced less thiocholine, which causes the decrease in its oxidation peak at +0.55 V. Optimum condition for carbofuran detection using CF/Graphene/Au was found to be at pH 7.4 and using 50 mU AChE, with 10 minutes contact time between ACTI and AChE, and 15 minutes inhibition time. Based on the CV experiments, the presence of Au particles accelerated the electron transfer rate and enhanced the sensitivity of the biosensor. The limit of detection (LOD) of biosensors for carbofuran detection is 8.08 μM and sensitivity measurement 0.3874 mA μM^{-1} cm^{-2}. The fabricated biosensor system showed a fairly good level of precision with a relative standard deviation of 6.77%. Determination of carbofuran in a real sample was done and the recoveries are 111.30 % and 88.95 % which means further study is required to create a biosensor system for practical application.

Author Contribution
Conceptualization, R.K.P and Y.T.; Methodology, S.T.; Validation, R.K.P and A.R.S.; Formal Analysis, A.R.S; Investigation, S.T. and A.R.S; Data Curation, R.K.P and Y.T.; Writing – Original Draft Preparation, S.T.; Writing – Review & Editing, A.R.S; Supervision, R.K.P. and Y.T.; Project Administration, R.K.P and A.R.S; and Funding Acquisition, R.K.P and Y.T.

Ethical Review Board Statement
Not available.

Informed Consent Statement
Not available.

Data Availability Statement
Not available.

Conflicts of Interest
The authors declare no conflict of interest.

Open Access

References
Akyüz, D., & Koca, A. (2019). An electrochemical sensor for the detection of pesticides based on the hybrid of manganese phthalocyanine and polyaniline. *Sensors and Actuators B: Chemical*, *283*, 848-856. https://doi.org/10.1016/J.SNB.2018.11.155

Anggraini, L. E., Rahmawati, I., Nasution, M. A. F., Jiwanti, P. K., Einaga, Y., & Ivandini, T. A. (2023). Development of an acrylamide biosensor using guanine and adenine as biomarkers at boron-doped diamond electrodes: Integrated molecular docking and experimental studies. *Bulletin of the Chemical Society of Japan*, *96*(5), 420-428. https://doi.org/10.1246/bcsj.20230030

Baek, S. H., Roh, J., Park, C. Y., Kim, M. W., Shi, R., Kailasa, S. K., & Park, T. J. (2020). Cu-nanoflower decorated gold nanoparticles-graphene oxide nanofiber as electrochemical biosensor for glucose detection. *Materials Science and Engineering: C*, *107*, 110273. https://doi.org/10.1016/j.msec.2019.110273

Bhuvanagayathri, R., Daniel, D. K., & Nirmala, G. (2020). Kinetic Evaluation of the Inhibition of Acetylcholinesterase for Use as a Biosensor. *ASEAN Journal of Chemical Engineering, 20*(1), 99-108. https://doi.org/10.22146/ajche.56709

Buglione, L., Chng, E. L. K., Ambrosi, A., Sofer, Z., & Pumera, M. (2012). Graphene materials preparation methods have dramatic influence upon their capacitance. *Electrochemistry Communications*, *14*(1), 5-8. https://doi.org/10.1016/j.elecom.2011.09.013

Cai, J., & Du, D. (2008). A disposable sensor based on immobilization of acetylcholinesterase to multiwall carbon nanotube modified screen-printed electrode for determination of carbaryl. *Journal of Applied Electrochemistry*, *38*, 1217-1222. https://doi.org/10.1007/s10800-008-9540-4

Cui, H. F., Wu, W. W., Li, M. M., Song, X., Lv, Y., & Zhang, T. T. (2018). A highly stable acetylcholinesterase biosensor based on chitosan-TiO$_2$-graphene nanocomposites for detection of organophosphate pesticides. *Biosensors and Bioelectronics*, *99*, 223-229. https://doi.org/10.1016/j.bios.2017.07.068

Dhull, V., Gahlaut, A., Dilbaghi, N., & Hooda, V. (2013). Acetylcholinesterase biosensors for electrochemical detection of organophosphorus compounds: a review. *Biochemistry research international*, *2013*(1), 731501. https://doi.org/10.1155/2013/731501

Díaz, A. N., & Peinado, M. R. (1997). Sol-gel cholinesterase biosensor for organophosphorus pesticide fluorimetric analysis. *Sensors and Actuators B: Chemical*, *39*(1-3), 426-431. https://doi.org/10.1016/s0925-4005(97)00025-7

Dong, P., Jiang, B., & Zheng, J. (2019). A novel acetylcholinesterase biosensor based on gold nanoparticles obtained by electroless plating on three-dimensional graphene for detecting organophosphorus pesticides in water and vegetable samples. *Analytical Methods*, *11*(18), 2428-2434. https://doi.org/10.1039/c9ay00549h

Eprilia, N., Sanjaya, A. R., Pramadewandaru, R. K., Pertiwi, T. A., Putri, Y. M., Rahmawati, I., ... & Ivandini, T. A. (2024). Preparation of nickel foam modified by multiwalled hollow

spheres of $NiCo_2O_4$ as a promising non-enzymatic glucose sensor. *RSC advances*, *14*(15), 10768-10775. https://doi.org/10.1039/d3ra08663a

Fatah, F. R., Sitorus, R., Saefumillah, A., Mubarok, H., & Pramadewandaru, R. K. (2024). Advanced electrochemical detection of arsenic using platinum-modified boron-doped diamond by anodic stripping voltammetry. *Environmental and Materials*, *2*(1), 61-76. https://doi.org/10.61511/eam.v2i1.2024.993

Fukuto, T. R. (1990). Mechanism of action of organophosphorus and carbamate insecticides. *Environmental health perspectives*, *87*, 245-254. https://doi.org/10.1289/ehp.9087245

Ivandini, T. A., Saepudin, E., Wardah, H., Harmesa, Dewangga, N., & Einaga, Y. (2012). Development of a biochemical oxygen demand sensor using gold-modified boron doped diamond electrodes. *Analytical chemistry*, *84*(22), 9825-9832. https://doi.org/10.1021/ac302090y

Jirasirichote, A., Punrat, E., Suea-Ngam, A., Chailapakul, O., & Chuanuwatanakul, S. (2017). Voltammetric detection of carbofuran determination using screen-printed carbon electrodes modified with gold nanoparticles and graphene oxide. *Talanta*, *175*, 331-337. https://doi.org/10.1016/j.talanta.2017.07.050

Khalil, I., Julkapli, N. M., Yehye, W. A., Basirun, W. J., & Bhargava, S. K. (2016). Graphene–gold nanoparticles hybrid—synthesis, functionalization, and application in a electrochemical and surface-enhanced raman scattering biosensor. *Materials*, *9*(6), 406. https://doi.org/10.3390/ma9060406

Khodadadi, A., Faghih-Mirzaei, E., Karimi-Maleh, H., Abbaspourrad, A., Agarwal, S., & Gupta, V. K. (2019). A new epirubicin biosensor based on amplifying DNA interactions with polypyrrole and nitrogen-doped reduced graphene: experimental and docking theoretical investigations. *Sensors and actuators b: chemical*, *284*, 568-574. https://doi.org/10.1016/j.snb.2018.12.164

Ma, C. B., Qi, X., Chen, B., Bao, S., Yin, Z., Wu, X. J., ... & Zhang, H. (2014). MoS_2 nanoflower-decorated reduced graphene oxide paper for high-performance hydrogen evolution reaction. *Nanoscale*, *6*(11), 5624-5629. https://doi.org/10.1039/c3nr04975b

Ma, L., Zheng, M., Liu, S., Li, Q., You, Y., Wang, F., ... & Shen, W. (2016). Synchronous exfoliation and assembly of graphene on 3D $Ni(OH)_2$ for supercapacitors. *Chemical Communications*, *52*(91), 13373-13376. https://doi.org/10.1039/c6cc07645a

Ma, Y., Song, X., Ge, X., Zhang, H., Wang, G., Zhang, Y., & Zhao, H. (2017). In situ growth of α-Fe_2O_3 nanorod arrays on 3D carbon foam as an efficient binder-free electrode for highly sensitive and specific determination of nitrite. *Journal of materials chemistry A*, *5*(9), 4726-4736. https://doi.org/10.1039/c6ta10744c

Massoulie, J., & Bon, S. (1982). The molecular forms of cholinesterase and acetylcholinesterase in vertebrates. *Annual review of neuroscience*, *5*(1), 57-106. https://doi.org/10.1146/annurev.ne.05.030182.000421

Nahda, D. P., Sanjaya, A. R., Rahmawati, F., Zulfia, A., Sumbodja, A., Pramadewandaru, R. K., ... & Ivandini, T. A. (2025). Synthesis of mesoporous carbon from banana peels with silica gel 60 as the hard templates. *RSC advances*, *15*(6), 4536-4545. https://doi.org/10.1039/d4ra08322a

Nunes, E. W., Silva, M. K., Rascón, J., Leiva-Tafur, D., Lapa, R. M., & Cesarino, I. (2022). Acetylcholinesterase biosensor based on functionalized renewable carbon platform for detection of carbaryl in food. *Biosensors*, *12*(7), 486. https://doi.org/10.3390/bios12070486

Olkhov, R. V., & Shaw, A. M. (2014). Growth kinetics of gold nanoparticles on silica/graphene surfaces for multiplex biological immunoassays. *RSC Advances*, *4*(60), 31678-31684. https://doi.org/10.1039/c4ra02326a

Ostadakbari, F., Yazdian, F., Rashedi, H., Ghaemi, A., Haghirosadat, B. F., & Azizi, M. (2021). Fabrication of a Sensitive Biosensing System for Cu^{2+} ion Detection by Gold-Decorated Graphene Oxide Functionalized with Gly-Gly-His. *Journal of Cluster Science*, *33*(6), 2617–2624. https://doi.org/10.1007/s10876-021-02169-3

Pino, F., Ivandini, T. A., Nakata, K., Fujishima, A., Merkoçi, A., & Einaga, Y. (2015). Magnetic enzymatic platform for organophosphate pesticide detection using boron-doped diamond electrodes. *analytical sciences*, *31*(10), 1061-1068. https://doi.org/10.2116/analsci.31.1061

Prasad, R., Upadhyay, N., & Kumar, V. (2013). Simultaneous determination of seven carbamate pesticide residues in gram, wheat, lentil, soybean, fenugreek leaves and apple matrices. *Microchemical Journal*, *111*, 91–96. https://doi.org/10.1016/j.microc.2012.12.014

Pundir, C. S., & Chauhan, N. (2012). Acetylcholinesterase inhibition-based biosensors for pesticide determination: A review. *Analytical biochemistry*, *429*(1), 19-31. https://doi.org/10.1016/j.ab.2012.06.025

Rachmawati, A., Sanjaya, A. R., Putri, Y. M. T. A., Gunlazuardi, J., & Ivandini, T. A. (2023). An acetylcholinesterase-based biosensor for isoprocarb using a gold nanoparticles-polyaniline modified graphite pencil electrode. *Analytical Sciences*, *39*(6), 911-923. https://doi.org/10.1007/S44211-023-00296-7/TABLES/4

Rahmawati, I., Einaga, Y., Ivandini, T. A., & Fiorani, A. (2022). Enzymatic biosensors with electrochemiluminescence transduction. *ChemElectroChem*, *9*(12), e202200175. https://doi.org/10.1002/celc.202200175

Ribeiro, E. B., Ribeiro, D. B., dos Santos Soares, A. M., Marques, P. R. B., Badea, M., Targa, M., ... & Nunes, G. S. (2022). A novel glutathione-S-transferase-based biosensor for pyrethroid insecticides: From inhibition study to detection. *Sensors and Actuators Reports*, *4*, 100093. https://doi.org/10.1016/j.snr.2022.100093

Sanjaya, A. R., Riyanto, H. G., Rahmawati, I., Putri, Y. M. T. A., Nurhalimah, D., Saepudin, E., ... & Krisnandi, Y. K. (2023). Carbon-coated nickel foam for hypochlorous acid sensor. *Environmental and Materials*, *1*(1). https://doi.org/10.61511/eam.v1i1.2023.105

Singh, A. P., Balayan, S., Hooda, V., Sarin, R. K., & Chauhan, N. (2020). Nano-interface driven electrochemical sensor for pesticides detection based on the acetylcholinesterase enzyme inhibition. *International Journal of Biological Macromolecules*, *164*, 3943-3952. https://doi.org/10.1016/j.ijbiomac.2020.08.215

Sookhakian, M., Mat Teridi, M. A., Tong, G. B., Woi, P. M., Khalil, M., & Alias, Y. (2021). Reduced graphene oxide/copper nanoparticle composites as electrochemical sensor materials for nitrate detection. *ACS Applied Nano Materials*, *4*(11), 12737-12744. https://doi.org/10.1021/acsanm.1c03351

Upadhyay, S., Rao, G. R., Sharma, M. K., Bhattacharya, B. K., Rao, V. K., & Vijayaraghavan, R. (2009). Immobilization of acetylcholineesterase–choline oxidase on a gold–platinum bimetallic nanoparticles modified glassy carbon electrode for the sensitive detection of organophosphate pesticides, carbamates and nerve agents. *Biosensors and Bioelectronics*, *25*(4), 832-838. https://doi.org/10.1016/j.bios.2009.08.036

Wang, K., Liu, Q., Dai, L., Yan, J., Ju, C., Qiu, B., & Wu, X. (2011). A highly sensitive and rapid organophosphate biosensor based on enhancement of CdS–decorated graphene nanocomposite. *Analytica Chimica Acta*, *695*(1-2), 84-88. https://doi.org/10.1016/j.aca.2011.03.042

Wang, M., Huang, J., Wang, M., Zhang, D., & Chen, J. (2014). Electrochemical nonenzymatic sensor based on CoO decorated reduced graphene oxide for the simultaneous determination of carbofuran and carbaryl in fruits and vegetables. *Food chemistry*, *151*, 191-197. https://doi.org/10.1016/j.foodchem.2013.11.046

Wei, M., Zeng, G., & Lu, Q. (2014). Determination of organophosphate pesticides using an acetylcholinesterase-based biosensor based on a boron-doped diamond electrode modified with gold nanoparticles and carbon spheres. *Microchimica Acta*, *181*, 121-127. https://doi.org/10.1007/s00604-013-1078-4

Yao, Y., Wang, G., Chu, G., An, X., Guo, Y., & Sun, X. (2019). The development of a novel biosensor based on gold nanocages/graphene oxide–chitosan modified acetylcholinesterase for organophosphorus pesticide detection. *New Journal of Chemistry*, *43*(35), 13816-13826. https://doi.org/10.1039/c9nj02556a

Zahirifar, F., Rahimnejad, M., Abdulkareem, R. A., & Najafpour, G. (2019). Determination of Diazinon in fruit samples using electrochemical sensor based on carbon nanotubes modified carbon paste electrode. *Biocatalysis and Agricultural Biotechnology*, *20*, 101245. https://doi.org/10.1016/j.bcab.2019.101245

Zhang, J., & Lee, H. K. (2006). Application of liquid-phase microextraction and on-column derivatization combined with gas chromatography–mass spectrometry to the determination of carbamate pesticides. *Journal of Chromatography A*, *1117*(1), 31-37. https://doi.org/10.1016/j.chroma.2006.03.102

Biographies of Authors

Respati Kevin Pramadewandaru, Department of Materials and Metallurgical Engineering, Faculty of Industrial Technology and System Engineering, Sepuluh Nopember Institute of Technology, Surabaya, East Java 60111, Indonesia.
- Email: respatikevin@its.ac.id
- ORCID: 0000-0002-8313-1596
- Web of Science ResearcherID: N/A
- Scopus Author ID: 57214135665
- Homepage: https://www.its.ac.id/tmaterial/id/respati-2/

Sulis Triani, Department of Chemistry, Faculty of Mathematics and Natural Sciences, Universitas Indonesia, Depok, West Java 16424, Indonesia.
- Email: sulistriani@ui.ac.id
- ORCID: N/A
- Web of Science ResearcherID: N/A
- Scopus Author ID: N/A
- Homepage: N/A

Yudisthira Tesla, Singota Solutions, Bloomington, Indiana 47401, United States.
- Email: yudistiratesla.singota@gmail.com
- ORCID: 0000-0002-7034-1113
- Web of Science ResearcherID: N/A
- Scopus Author ID: 57192371075
- Homepage: N/A

Afiten Rahmin Sanjaya, Department of Chemistry, Faculty of Mathematics and Natural Sciences, Universitas Indonesia, Depok, West Java 16424, Indonesia.
- Email: afiten.rahmin@ui.ac.id
- ORCID: 0000-0001-6834-4588
- Web of Science ResearcherID: ISB-6405-2023
- Scopus Author ID: 58117944600
- Homepage: N/A